Some numerical relativity methods for grazing black holes using hierarchical 3+1 decomposition of Einstein's equations

Samuel Rocha de Oliveira

28th February 2003

Depto. de Matemática Aplicada, UNICAMP

1 Introduction

Let the the space-time metric be

$$\widetilde{g}_{\mu\nu} = \exp(2\Omega) \left\{ \begin{array}{cc} \left[-N^2 + \left(\gamma^{ij} b_i b_j\right)\right] & \exp(\Psi) b_j \\ \exp(\Psi) b_i & \exp(2\Psi)\gamma_{ij} \end{array} \right\},$$

Figure 1: Linux X Ruindows

where the factored spatial metric is

$$\gamma_{ij} = \begin{pmatrix} A^2 + \sigma^{IJ} c_J c_J & \exp(\Sigma) c_J \\ \exp(\Sigma) c_I & \exp(2\Sigma)\sigma_{IJ} \end{pmatrix}.$$

We further decompose the bi-dimensional metric σ_{IJ} as follows:

$$\sigma_{IJ} = \begin{pmatrix} B^2 + d^2 & Cd \\ Cd & C^2 \end{pmatrix}.$$

13 metric functions: $N, A, B, C, \Omega, \Psi, \Sigma, b_i, c_J, d$.

This decomposition allows the control of

$$\det(\widetilde{g}) = -\left(NABC\right)^2 \exp\left(8\Omega + 6\Psi + 4\Sigma\right),$$

where the usual coordinates singularities appears.

Note also that

$$\begin{aligned} \det(\gamma) &= \left(ABC\right)^2 \exp\left(4\Sigma\right), \\ \det(\sigma) &= \left(BC\right)^2. \end{aligned}$$

Thus, none of the "covectors" b_i, c_J, d affect the volume element.

These covectors are defined in the natural cotangent space of the manifolds (M^3, γ), (M^2, σ) and $(M^1, 1)$ respectively. Some topological restrictions!

The "scale" functions of the "principal" directions have to be positive definite

Greek indices, like μ ranges the spacetime dimensions (0..3), lower case latin indices, like i, ranges the space dimensions (1..3) and the upper case latin indices like I ranges the surface indices $(2, 3)$.

and bounded:

$$N, A, B, C > 0$$

The other functions may vanish but have to be bounded as well.

$$|\Omega, \Psi, \Sigma, b_i, c_J, d| < \infty$$

There are only six of dynamical functions.

The initial boundary value problem for General Relativity requires the solution for the constraints equations:

$$\widetilde{G}_{t\mu} = \kappa \widetilde{T}_{t\mu}$$

for the dynamic functions and their first time derivatives.

Then the evolution equations:

$$\widetilde{G}^j_i = \kappa \widetilde{T}^j_i$$

evolve the dynamical functions along time. They are coupled second order in time.

At the outer FINITE boundary we have to solve the constraints

$$\widetilde{G}^\mu_{\text{normal}} = \kappa \widetilde{T}^\mu_{\text{normal}}$$

for some of the functions and their normal derivatives. This is different from the usual Dirichlet, Neuman or radiation boundary conditions.

These choices imply the 4-vectors along each direction $1, 2, 3$ be space-like and it cannot change the behavior to become null or time-like. Similarly the 4-vector along the direction 0 is always time-like and infinite red-shifts are avoided. Of course, some of the observers will hit the curvature singularities in a finite time and have to be discarded. The coordinates and naked singularities are eliminated from either the computational grid or from the equations themselves, as much as possible, with the aid of the extra functions.

Let us call dynamical functions those which the Einstein equations give second order derivative in time.

Let us restrit to the vacuum case:

$$\widetilde{T}_{\alpha\beta} = 0.$$

2 Numerical Analysis

2.1 Boundary Value Problem: Initial Data

2.1.1 Linearization

Our general boundary value problem can be cast as the following set of second order quasi-linear coupled equations (*gBV2oqlpdes*):

$$\mathbf{A}_{dc}^{ab}[x]\left(\partial_a\left(V_e^c\partial_b U^e\right)\right) + \mathbf{F}_d\left[\left(\partial_b U^e\right), U^c, x\right] = 0 \qquad x \in \Xi,$$

for a list of functions $U^e[x]$ and the boundary equations:

$$\mathbf{B}_d\left[\left(\partial_n U^e\right), U^c, x\right] = 0 \qquad x \in \partial\Xi,$$

where $(\partial_n U^e)$ is the normal derivative of $U^e[x]$. We use the standard summation on repeated indexes for the appropriate ranges. The non singular arrays $\mathbf{A}$ and $\mathbf{V}$ are given functions of the position x; $\mathbf{F}$ and $\mathbf{B}$ are, in general, non-linear functions of their arguments.

We start from an initial guess for the functions, and a (Newton) linearization

around the guesses:

$$U^e_{improved}[x] = U^e_{guess}[x] + u^e[x]$$

2.1.2 Discretization

The linearized differential equations for $u^e[x]$ go through a second order accuracy estimate of the integral in a adjustable finite volume around every grid point of Ξ and $\partial\Xi$.

Since the differencing is done in three dimensions and all mixed derivatives are involved, we have stencils with 19 to 27 points grid point not on the boundary.

On the boundary the stencils are centered on the 2 dimensional surface plus upward or inward difference scheme with 6 to 12 points.

The algebraic equations are generate with Maple.

2.1.3 Linear sistem

The **linear algebraic equations** are solved by Gauss-Seidel methods.

The order of the linear sistem is:

[Number of functions $u^e[x]$] x [number of points in the closed grid] $\approx 4 \times 20 \times 20 \times 10 = 16000$

The number of operations for the solution of the linear problem by Gauss-Seidel methods till the error is below 10^{-4} is $\approx 2 \times 10^9$. About 10 seconds of CPU time with a single 200 MHz processor.

Figure 2: Finire volume for diferencing:

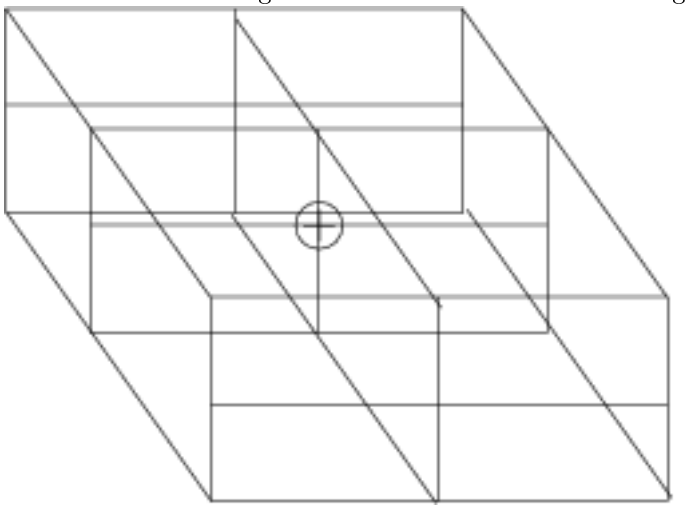

The process is iterated till a **convergence** criteria is met. Both Gauss-Seidel and Newton iterations.

For a 200 MHz cpu, each Gauss-Seidel solution takes about 10 seconds.

There are faster solvers for specific linear system classes. But we have mixed both the equations in the grid and at the boundaries so we can not have, in general, fixed band matrices, for example.

2.2 Initial Boundary Value Problem: The Evolution

The initial value boundary problem can be written as the set of second order quasi-linear coupled equations (*gIBV2oqlpdes*):

$$\mathbf{g}_{dc}^{\beta}\left[x,t\right]\left(\partial_t\left(V_e^c\partial_\beta U^e\right)\right)+\mathbf{A}_{dc}^{ab}\left[x,t\right]\left(\partial_a\left(V_e^c\partial_b U^e\right)\right)+\mathbf{F}_d\left[\left(\partial_b U^e\right),\left(\partial_t U^e\right),U^c,x,t\right]=0,$$

$x\in\Xi, t\in[0,T]$, for a list of functions $U^e\left[x,t\right]$ having the initial conditions:

$$U^e\left[x,0\right]=f^e[x],\quad \partial_t U^e\left[x,0\right]=h^e[x]$$

and the boundary equations:

$$\mathbf{B}_d\left[\left(\partial_n U^e\right),\left(\partial_t U^e\right),U^c,x\right]=0\qquad x\in\partial\Xi.$$

Similarly to the previous setting, the non singular arrays **A** and **V** are given functions of x and t; **F** and **B** are, in general, non-linear functions of their arguments and the index β allows both time and space differentiation.

At the moment our numerical scheme for the initial value boundary problem is a implicit, staggered, **second order in time and space, finite difference method** (Crank Nicholson like schemes). For non stiff problems we allow semi-implicit schemes with two iterations for each time step, otherwise the tri-diagonal linear problem is combined with a Newton linearization of the non-

linear terms with a Gauss-Seidel solver. The parameter space is considerably large and no attempts of automatic choices were made.

The boundary equations, eventually, has to be linearized around a guess. This is the most probable incoming of spurious modes. Even for simmetry boundaries!

3 Grazing Black Holes

The iteration process of the boundary value problem starts with the exact solution for two black holes (with conical singularities) in Weyl coordinates. See figures. So we prescribe, as free initial data, all the metric functions but c_J and $\partial_t c_J$. These four functions are the unknowns of the constraint equations.

The area of the one black hole's horizon,

$$A \approx M^2,$$

can not decrease, so the coalescence of two black holes will present a jumping in the final area of the horizon:

$$M \approx m_1 + m_2 A \approx M^2 > m_1^2 + m_2^2$$

3.1 Initial Data

The initial data is constructed solving the nonlinear constraint equations using analytical exact solutions superpositions for the free initial data.

Figure 3: Ilustration for the black hole initial data based on a particular Weyl solution

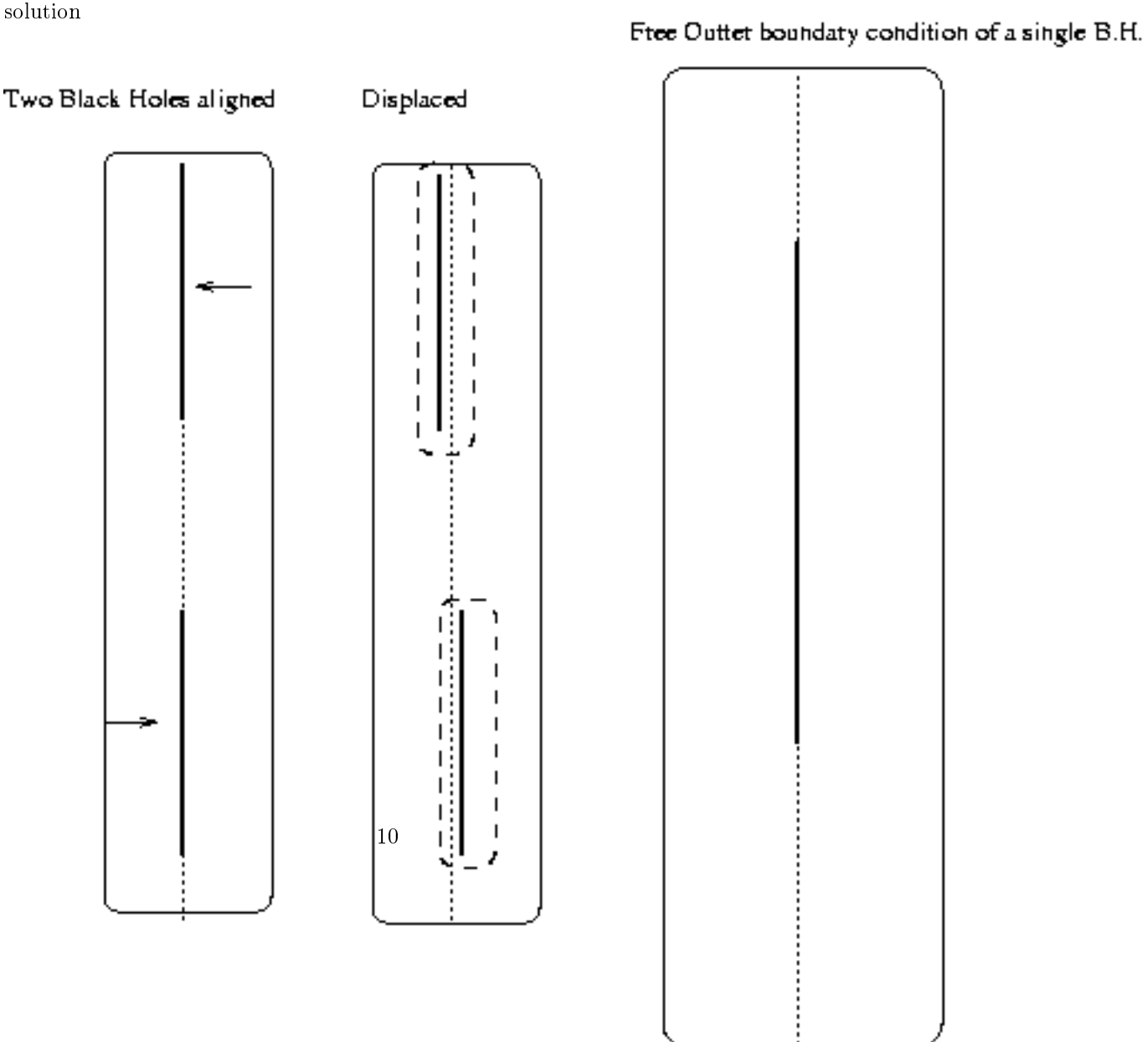

Figure 4: The Merger of apparent horizons in the simulations of Alcubierre et. al. (2001)

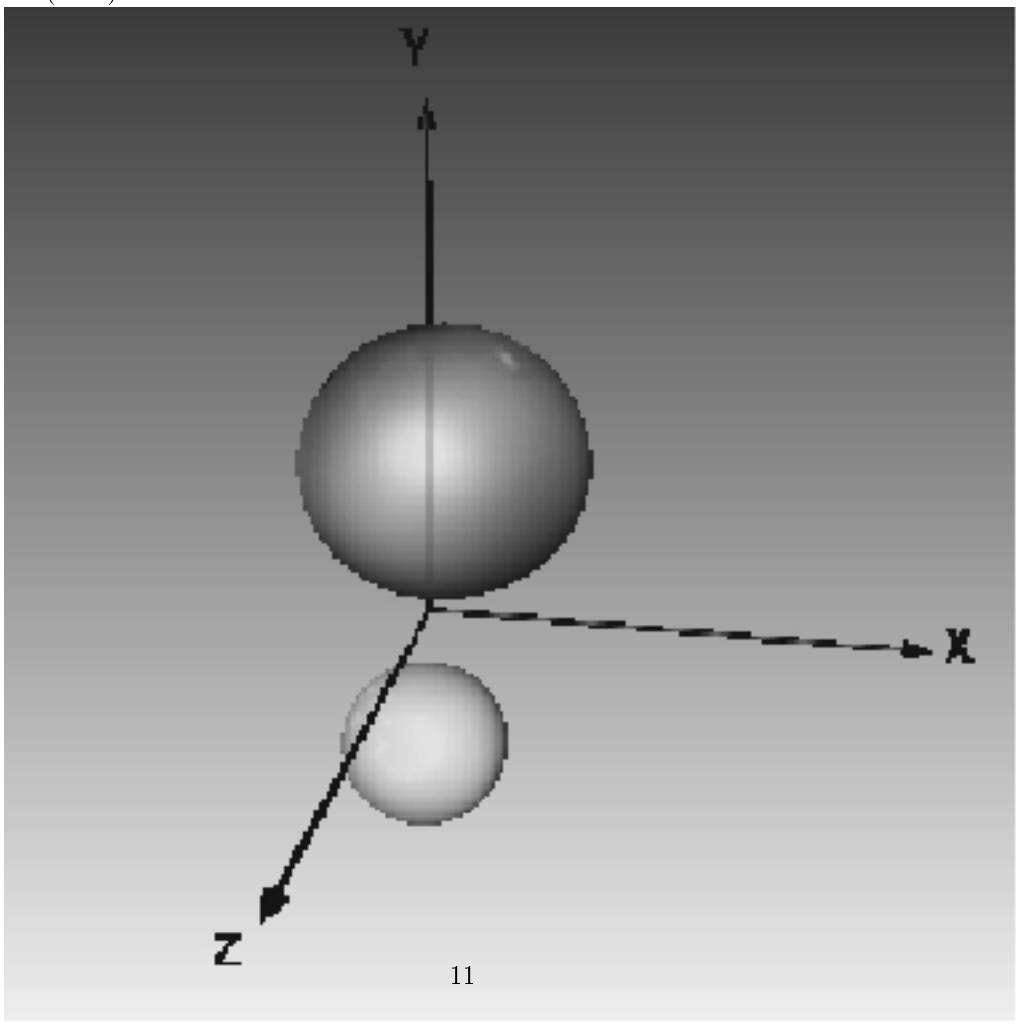

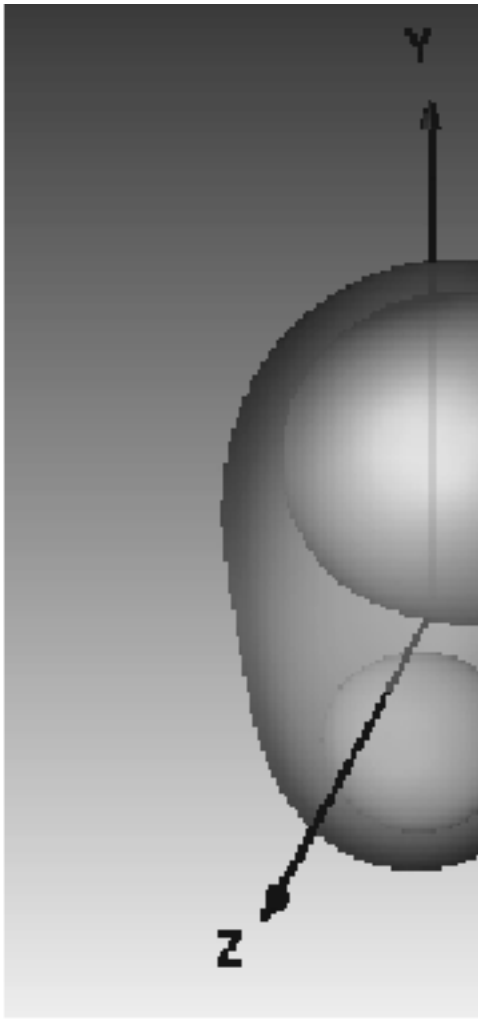

There remains 4 elliptical second order quasi-linear elliptical equations with non constant coefficients.

The are solved from an initial guess and relaxation of the elliptical equations using finite difference algebraic equations. The constraints are not solved any further. They are used as measure of accuracy during the evolution. The outer boundary conditions for the initial data are exact solutions of supposed configurations.

The fourth order differences provide more accurate solutions and propagate gravitational waves with less dispersion and damping than the second order differences. However, fourth order differences are more unstable than second order, particularly at late times in the evolution when large gradients develop near the horizon.

The outer boundary conditions for the initial data are exact solutions of supposed configurations: A final distorted black hole.

For the lapse function we chose a few variations of "1+log" slice.

For the shift vectors we use minimal distortion conditions on the factored metric. This expensive choice results in 3 more elliptical equations which have to be solved in every time step but it keeps the codes running longer.

3.2 Evolution

With respect to those observers the evolution equations are solved using second order (quasi) implicit finite difference/volume methods.

Richardson's extrapolations methods to show the second order of the code and to improve the accuracy.

At the outer boundaries we have a combination of standard Newman or radiation conditions and up to four of the Einstein equations as constraints on the conditions – for simplicity we either use an analytical exact solution or "tangential" linearized Einstein equations.

For inner boundary conditions (at the holes) we damp and freeze the functions close to the "singularities".

Let m the the total ADM like mass of the isolated system. Our code, nowadays, is running up to about $14m$ with the constraints L_2 violations below 1% for a grid size of the order of $m/8$ in each spatial direction and a time step equivalent to $m/32$. After that time spurious modes prevail. An estimate of the amount of gravitational wave energy emitted between the time $4m$ and $10m$ is below $10^{-4}m$. The horizons are not localized in our simulations yet. The dimensions of our grid for a typical run is $20 \times 20 \times 10 \times m^3$.

Grid crossing time...

4 Computational Details e Conclusions

Most of our code contains Fortran 77 standard subroutines, specially for linear algebra and ordinary differential equations. Several pieces of the code now are in Fortran 95 (Lahey compiler) and in C++ (gcc compiler). For several tasks we use Maple 7: (symbolic manipulation, code generation, grtensor, parameters manipulation etc.). No parallel implementation yet. Our codes are directly linked to simple graphics software (gnu-plot and octave) but we intend to use the recent Open DX (based on IBM's Visualization Data Explorer) which can

Figure 5: Hamitonian violation

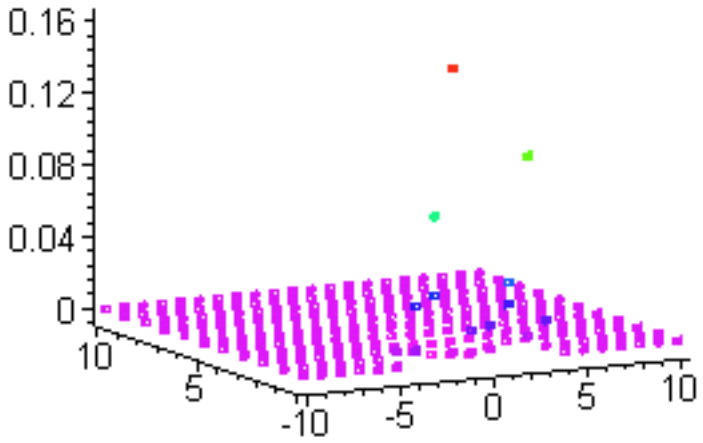

Figure 6: Einstein

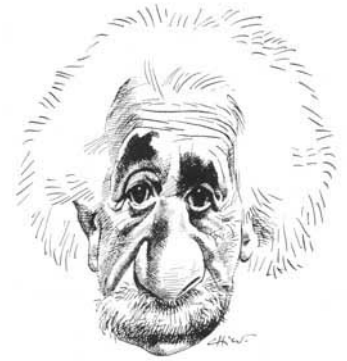

be linked to Fortran/Linux/X11 software.